J Therm Anal Calorim (2013) 111:1523–1530
DOI 10.1007/s10973-012-2480-6

Polymerization behavior and thermal properties of benzoxazine based on 4,4′-diaminodiphenyl ether

Yanfang Liu · Zhihong Li · Jian Zhang · Haili Zhang · Huiying Fan · Mingtao Run

Received: 7 November 2011 / Accepted: 7 May 2012 / Published online: 5 June 2012

Abstract The thermally activated ring-opening polymerization behavior of benzoxazine based on 4,4′-diaminodiphenyl ether was investigated by Fourier transform infrared and differential scanning calorimetry, and the thermal properties of the corresponding polybenzoxazine were studied by dynamic mechanical analysis, thermogravimetry-mass spectrometry, and differential thermal analysis. In the ring-opening polymerization reaction, the C–O–C absorption peak of the oxazine ring at 1,054 cm^{-1} disappeared first, and the C–N–C absorption intensity of the oxazine ring decreased gradually with time rising. The activation energies of the non-isothermal polymerization are 83.4 and 87.4 kJ mol^{-1} evaluated with Kissinger and Flynn–Wall–Ozawa methods, respectively. Dynamic mechanical analysis shows the glass transition temperature of the resultant polybenzoxazine is 188 °C. In the thermal degradation, the 10 % mass loss temperature of the polybenzoxazine is 353 °C and the char yield is about 48 % at 800 °C in nitrogen, while 415 °C and close to 0 % at 650 °C in air.

Keywords Benzoxazine · Ring-opening polymerization · Dynamic mechanical properties · Thermogravimetry-mass spectrometry · Thermal stability

Y. Liu (✉) · J. Zhang · H. Zhang · H. Fan · M. Run
College of Chemistry & Environmental Science, Hebei University, Baoding 071002, China
e-mail: liuyanfang@msn.com

Z. Li
Office of Educational Administration, Hebei University, Baoding 071002, China

Introduction

Benzoxazines are six-membered heterocyclic compounds synthesized via Mannich condensation reaction from phenols, amines, and formaldehyde. The first benzoxazine compound was synthesized by Holly and Cope in 1944 [1]. Later, the study on benzoxazines and their oligomers was further conducted from the 1950s to 1970s [2–7]. These benzoxazines were synthesized from monophenols, monoamines, and formaldehyde, but they could not form polymers with high molecular weight. After benzoxazines based on bisphenol-A were synthesized [8, 9], a series of bifunctional benzoxazines have been prepared from bisphenols (or monophenols), monoamines (or diamines), and formaldehyde [10–23]. The bifunctional benzoxazines can form into polybenzoxazines with high molecular weight via thermally activated ring-opening polymerization reaction [24–27], and the resultant polybenzoxazines possess excellent properties, such as relatively high glass transition temperature, superior mechanical properties, excellent electrical insulation properties, low moisture absorption, high thermal stability, high char yields, and low flammability. Therefore, benzoxazines can be used as high-performance matrices in electronics and aerospace industries.

Owing to the design flexibility for the molecular structure of benzoxazines, various benzoxazines with different structures were synthesized, and much effort has been devoted to investigating the properties of the resultant polybenzoxazines. The properties of polybenzoxazine materials mainly depend on the molecular structure of the corresponding benzoxazines. Recently, benzoxazines based on aromatic diamines attract the interest of many researchers, and 4,4′-diaminodiphenyl methane (DDM), 4,4′-diaminodiphenyl ether (DDE), and 4,4′-diaminodiphenyl sulfone

(DDS) were employed as starting materials to synthesize benzoxazines [14–23]. In the previous researches, a detailed study on benzoxazine based on 4-cyanophenol and DDE was reported [22], some DDE-based benzoxazines were mentioned as part of several compound study [18–21], while the benzoxazine based on phenol and DDE has not been studied comprehensively [21]. From the view of molecular structure, the bridging group between the aromatic rings is oxygen in DDE, methylene in DDM, and sulfone in DDS. As a bridging group, oxygen has the advantage of occupying small volume and possessing high flexibility for polybenzoxazine formed from DDE.

The objective of this study is to investigate the thermally activated ring-opening polymerization behavior of benzoxazine (P-DDE) based on DDE and the properties of the corresponding polybenzoxazine (PP-DDE). The ring-opening polymerization of P-DDE was studied with Fourier transform infrared (FTIR) spectroscopy and differential scanning calorimetry (DSC). The thermal properties and stability of PP-DDE were investigated by dynamic mechanical analysis (DMA), thermogravimetry (TG), thermogravimetry-mass spectrometry (TG-MS), and differential thermal analysis (DTA), respectively.

Experimental

Materials

4,4′-Diaminodiphenyl ether (DDE) was purchased from Shanghai Chemical Reagent Co., China. Phenol, formaldehyde (37 wt% aqueous), aniline, toluene, and chloroform were obtained from Tianjin Chemical Reagent Co., China. All chemicals were used as received.

Synthesis of P-DDE

To a 100 mL three-necked round bottom flask equipped with a mechanical stirrer, a thermometer, and a reflux condenser, 4.0 g (0.02 mol) DDE, 6.5 mL (0.08 mol) formaldehyde, and 20 mL toluene were added. The mixture was stirred for 1 h in an ice bath before adding the solution of 3.8 g (0.04 mol) phenol in 10 mL toluene. The temperature was then gradually raised to 90 °C, and the mixture was allowed to reflux for 24 h. Subsequently, the solution was poured into a separatory funnel and washed several times with 3 M NaOH aqueous solution and deionized water, respectively. Then, the solution was washed several times with 1 M HCl aqueous solution and deionized water, respectively. The solvent was removed by distillation under reduced pressure. Thereafter, it was dried at 70 °C in a vacuum oven for 6 h and then at 70 °C in an air circulated oven for 8 h, and a pale yellow powder was obtained. The yield was 70 %.

Preparation of PP-DDE

P-DDE was first heated to about 140 °C, and then was poured into a preheated steel mold. The mold was kept in a vacuum oven conditioned at 140 °C for 2 h to remove the entrapped air from the molten specimen and step-cured in an air-circulating oven at 200 °C for 2 h and 220 °C for 4 h.

Measurements

Both proton (^{1}H) and carbon (^{13}C) nuclear magnetic resonance (NMR) spectra were recorded by a Bruker Avance III 600 NMR spectrometer at a proton frequency of 600 MHz and the corresponding carbon frequency. Deuterated chloroform ($CDCl_3$) was used as a solvent and tetramethylsilane as an internal standard.

FTIR spectra were obtained with a Nicolet 380 FTIR spectrometer at a resolution of 4 cm^{-1}. P-DDE was dispersed in KBr and pressed the mixture into a disk. After scanned by the FTIR spectrometer, the disk was placed in an air-circulating oven with a fixed temperature. During the polymerization reaction, the disk was removed periodically for measurement.

The quantitative analyses of C, H, N, and O were carried out on an Exeter Analytical CE-440 elemental analyzer.

The non-isothermal polymerization reaction of P-DDE was monitored by a Shimadzu DSC-41 differential scanning calorimeter operating in a nitrogen atmosphere. The P-DDE samples of about 6.5 mg were scanned at five heating rates: 5, 7.5, 10, 12.5, and 15 °C min^{-1}, respectively. Besides, the glass transition temperature (T_g) of PP-DDE was determined by DSC at a heating rate of 20 °C min^{-1}.

A Perkin-Elmer DMA-8000 dynamic mechanical analyzer was used to determine the dynamic storage modulus (E'), loss modulus (E''), and loss factor (tan δ) of PP-DDE using the single cantilever bending mode. Measurement was performed from 25 to about 260 °C at a heating rate of 5 °C min^{-1} in static air atmosphere, and the testing frequency was set at 1 Hz. The dimension of the specimen was approximately 10.0 × 5.8 × 2.4 mm.

A Shimadzu TGA-40 thermogravimeter was used to determine the mass loss behavior of PP-DDE. The PP-DDE samples of about 3.4 mg were heated to 800 °C at a heating rate of 10 °C min^{-1} in dynamic nitrogen and static air atmospheres, respectively.

The composition of the gases released from thermal degradation of PP-DDE was determined by TG-MS, which was carried out on a Netzsch STA 449 C thermogravimeter coupled with a Netzsch QMS 403 C quadrupole mass

spectrometer. A quartz capillary was used to transfer gases from the gas outlet at the furnace of the thermobalance to the gas inlet at the mass spectrometer, and the capillary was kept at 250 °C. Mass spectra were recorded under an ionization voltage of 70 eV. The MS scan duration was set at 0.5 s, and the mass range for MS data acquisition was 2–100 atomic mass units. PP-DDE sample was heated from a room temperature up to 850 °C at a heating rate of 10 °C min^{-1} in the thermogravimeter in air.

A Shimadzu DTA-40 differential thermal analyzer was used to determine the heat release behavior of PP-DDE in the thermal degradation. The PP-DDE samples of about 14 mg were heated to 800 °C at a heating rate of 10 °C min^{-1} in dynamic nitrogen and static air atmospheres, respectively.

Results and discussion

Synthesis and characterization

P-DDE was synthesized from phenol, DDE and formaldehyde via a solution method [8], and the synthesis reaction mechanism is shown in Scheme 1. The chemical structure of P-DDE was confirmed with ^{1}H and ^{13}C NMR, FTIR, and element analysis.

The ^{1}H NMR spectrum of P-DDE is shown in Fig. 1. The resonances appearing at 4.54 ppm and 5.27 ppm are assigned to the methylene protons (H7 and H8) of Ar–CH_2–N and O–CH_2–N of the oxazine ring, respectively. The chemical shifts (ppm) at 6.78–6.80 (2H, H3), 6.83–6.86 (4H, H10), 6.86–6.88 (2H, H4), 6.96, 6.98 (2H, H2), 7.01–7.04 (4H, H11), 7.10 (2H, H1) are assigned to the aromatic protons. The ratio of the corresponding integration areas of the eight protons (H1, H2, H3, H4, H7, H8, H10, and H11) was determined roughly to be 1:1:1:1:2:2:2:2, which is well coincident with the theoretical proton ratio based on the chemical structure.

In the corresponding ^{13}C NMR spectrum shown in Fig. 2, the resonances appearing at 50.99 ppm and 80.25 ppm are assigned to the methylene carbons (C7 and C8) of Ar–CH_2–N and O–CH_2–N of the oxazine ring, respectively. Other chemical shifts (ppm) are assigned to

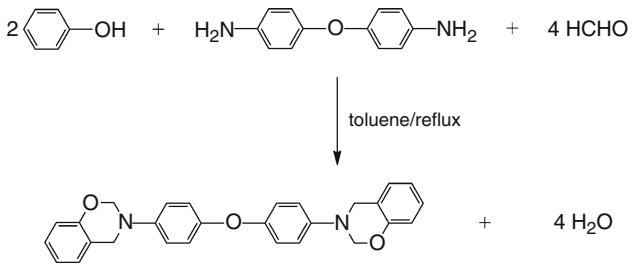

Scheme 1 Chemical reaction of P-DDE monomer synthesis

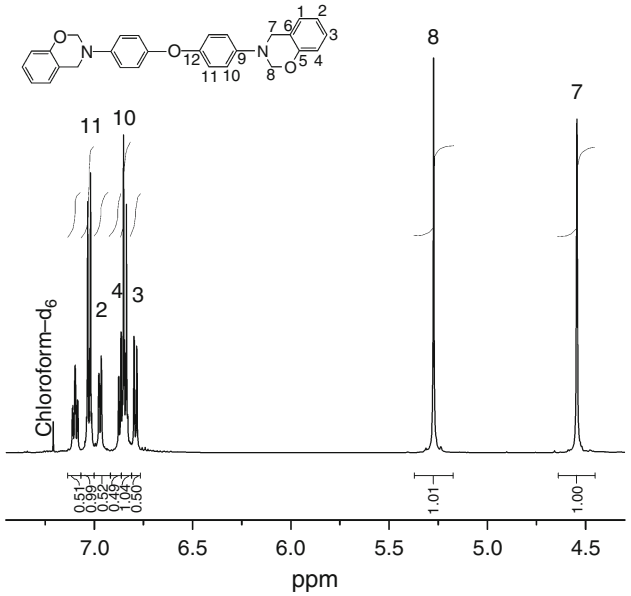

Fig. 1 ^{1}H NMR spectrum of P-DDE monomer

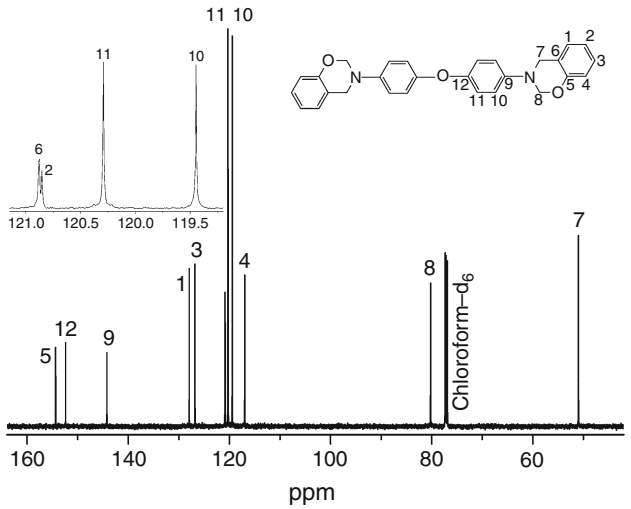

Fig. 2 ^{13}C NMR spectrum of P-DDE monomer

the resonances of the aromatic carbons: 116.97 (C4), 119.45 (C10), 120.30 (C11), 120.86 (C2), 120.88 (C6), 126.81 (C3), 127.96 (C1), 144.24 (C9), 152.39 (C12), 154.38 (C5).

Elemental analysis of P-DDE shows that the experimental results (C, 77.15 %; H, 5.43 %; N, 6.59 %; O, 10.83 %) are consistent with the theoretical values (C, 77.06 %; H, 5.50 %; N, 6.42 %; O, 11.01 %).

The FTIR spectrum of P-DDE is shown in Fig. 3a. The characteristic absorptions at 1158 and 1,116 cm^{-1} are assigned to the asymmetric stretching vibrations of C–N–C, while the absorption peak at 872 cm^{-1} corresponds to the symmetric stretching vibration of C–N–C [28]. The asymmetric stretching vibration of C–O–C is observed at

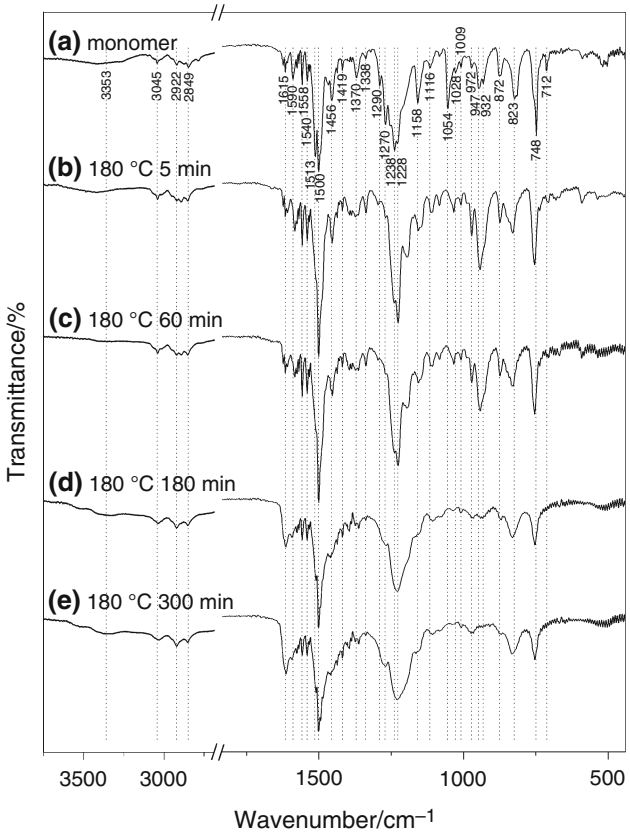

Fig. 3 FTIR spectra of *a* P-DDE monomer and *b–e* polymerization products obtained at 180 °C in air for different times

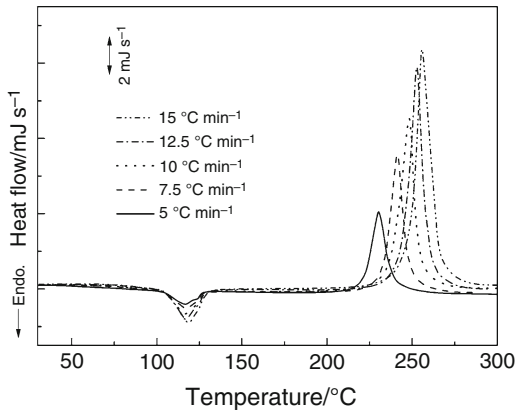

Fig. 4 Non-isothermal DSC curves of P-DDE at different heating rates

1238 cm^{-1}, and the symmetric stretching vibrations of C–O–C are observed at 1,054 and 1,028 cm^{-1} [28]. The absorptions at 972, 947, and 932 cm^{-1} are the characteristic modes of the benzene ring with an oxazine ring attached. The peaks at 1290, 1270, 1228, and 1009 cm^{-1} are due to the stretching vibrations of Ar–O–Ar. The absorptions at 1622, 1615, 1590, 1558, 1540, 1513, 1500, and 1456 cm^{-1} are associated with the C=C stretching vibrations of the aromatic ring. The band at 1,338 cm^{-1} is assigned to the C–H in-plane bending of the aromatic ring, and the C–H out-of-plane bending of the aromatic ring can be found at 823 and 748 cm^{-1}. Besides, the C–H stretching vibration of the aromatic ring appeared at 3,045 cm^{-1}, and the C–H asymmetric and symmetric stretching vibrations of CH_2 of the oxazine ring are at 2,922 and 2,849 cm^{-1}, respectively. The absorption peaks at bands of 1419, 1370, and 712 cm^{-1} are due to the CH_2 scissoring, wagging, and rocking vibrations of the oxazine ring, respectively. The FTIR spectrum of P-DDE is consistent with the proposed structure.

Ring-opening polymerization behavior

The structure changes of P-DDE in the thermally activated ring-opening polymerization were studied by FTIR, and the FTIR spectra of the polymerized product obtained at 180 °C for different times in air are shown in Fig. 3b–e. With the beginning of the ring-opening polymerization reaction, the absorption peak of C–O–C at 1,054 cm^{-1} vanished in 5 min, indicating that the oxazine rings have been opened. Meanwhile, the absorption intensities of the asymmetric and symmetric stretching vibrations of C–N–C at 1,158 and 872 cm^{-1}, and the CH_2 rocking vibrations of the oxazine ring at 712 cm^{-1} decreased gradually. Moreover, the characteristic absorption peaks of the benzene ring with an oxazine ring attached at 972 and 947 cm^{-1} increased in 5 min, then decreased, and disappeared in 300 min. Correspondingly, due to the ring-opening polymerization reaction, the intensities of the absorptions at 1590, 1558, 1540, 1500, 1456, 1338, 1238, 1228, 1116, 1028, 972, 947, and 932 cm^{-1} first increased in 5 min and then decreased gradually, while the intensities of the absorptions at 823 and 748 cm^{-1} first decreased and then maintained at a certain value. In addition, the intensity of the absorption at 1,615 cm^{-1} increased gradually with the reaction time rising, and the broad peak appeared around 3,353 cm^{-1} is ascribed to the stretching vibration of phenolic OH group formed in the ring-opening process.

The heat release behavior of benzoxazines in thermally activated ring-opening polymerization is generally studied by DSC [10, 11, 14, 16, 24, 29–31], and non-isothermal DSC mode is a commonly used method. The non-isothermal DSC curves of P-DDE at different heating rates are shown in Fig. 4. As can be seen, an endothermic peak appeared in the temperature range from about 108 to 125 °C corresponding to the melting process of P-DDE. With the temperature rising, an exothermic reaction peak was observed over the temperature range of 215–265 °C, which is ascribed to the polymerization reaction of P-DDE. The endothermic heat for P-DDE melting is 48 J g^{-1} and the exothermic heat for P–DDE polymerization is 262 J g^{-1}, which are lower than those of the 4-cyanophenol based

Table 1 Peak temperatures and kinetic parameter values obtained from non-isothermal DSC curves

Heating rate/°C min^{-1}	T_p/°C	Kissinger		Flynn–Wall–Ozawa/E/kJ mol^{-1}
		E/kJ mol^{-1}	A/s^{-1}	
5	230.2	83.4	8.6×10^4	87.4
7.5	241.0			
10	248.8			
12.5	253.2			
15	255.8			

benzoxazine [22]. The temperature of the thermal assisted polymerization is higher than that of some benzoxazines [10, 11, 14, 16, 24, 29–31]. Based on the difference in the exothermic peak temperatures (T_p) at several heating rates, the reaction kinetic parameters were determined by Kissinger and Flynn–Wall–Ozawa methods [32–34].

Kissinger's technique assumes that the maximum reaction rate occurs at peak temperatures [32], where $d^2\alpha/dt^2 = 0$, and it can be expressed as follows

$$\ln\left(\frac{\beta}{T_p^2}\right) = \ln\left(\frac{AR}{E}\right) - \frac{E}{RT_p} \quad (1)$$

where β is the linear heating rate, A is the pre-exponential factor, E is the activation energy, and R is the universal gas constant. Therefore, a plot of $\ln(\beta/T_p^2)$ versus $1/T_p$ gives the values of E and A.

Flynn–Wall–Ozawa method assumes that the degree of conversation at peak temperatures for different heating rates is a constant [33, 34], and it can be expressed as follows

$$\ln\beta = -1.052\frac{E}{RT} + C \quad (2)$$

where C is a constant, T is the iso-conversion temperature, and the other parameters are the same as described previously. E can be obtained from the slope of the plot of $\ln\beta$ versus $1/T_p$.

According to Eqs. 1 and 2, the polymerization kinetic parameters were calculated, and the results are listed in Table 1.

The activation energy values of P-DDE are lower than those of benzoxazines based on phenols with an electron-withdrawing group [10, 17, 35], but close to or higher than those of benzoxazine formed from phenol with an electron-donating group [24, 36]. In general, the thermally activated polymerization of benzoxazine is thought to proceed with a cationic ring-opening reaction, and the activation energy of the reaction depends on the molecular structures of benzoxazines. If there is an electron-donating substitute on the aromatic ring with which the oxazine ring attached, the electron cloud density of the aromatic ring will be increased, which will increase the reactivity of the aromatic hydrogens at the ortho and para positions and decrease the ring-opening polymerization reaction energy. While for an electron-withdrawing substitute, things will be in the opposite direction. Therefore, affected by the electron effect generated from the substitute on the aromatic ring of the phenolic backbone unit in benzoxazines, the activation energy of the ring-opening reaction will be increased or decreased.

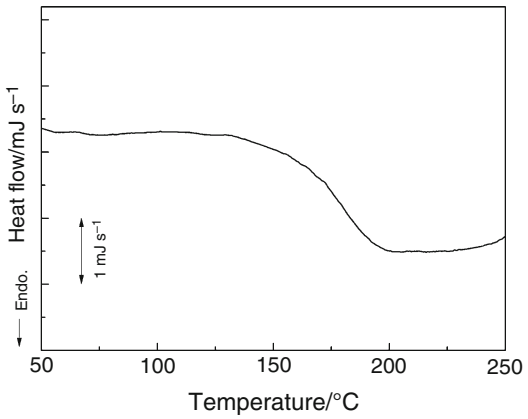

Fig. 5 DSC curve of PP-DDE

In addition, the DSC curve of PP-DDE is shown in Fig. 5, and the T_g of PP-DDE is 176 °C.

Dynamic mechanical properties

The temperature dependence of E', E'', and tan δ for PP-DDE are shown in Fig. 6. The E' is around 4.9 GPa at room temperature (25 °C) implying higher stiffness than that of polybenzoxazine based on 4,4′-diaminodiphenyl sulfone (PP-DDS) [23], which may be attributed to the difference in molecular structure between PP-DDE and PP-DDS. Oxygen is the bridging group between the aromatic rings of the phenolic backbone unit in PP-DDE while sulfone group in PP-DDS. The oxygen bridge occupies smaller volume in PP-DDE than sulfone group in PP-DDS. Besides, the oxygen bridge is more flexible than sulfone group, and the aromatic rings linked by oxygen in PP-DDE can rotate freely, while those linked by sulfone in PP-DDS cannot for the rigidity of O=S=O. Therefore, PP-DDE molecule possess a higher degree of conformational flexibility than PP-DDS molecule, and PP-DDE molecule can reach a more stable conformational state below T_g than PP-DDS molecule. Consequently, the E' of PP-DDE is higher than that of PP-DDS at room temperature. With the temperature rising, E' started to decrease at about 150 °C with T_g of 188 °C determined from the peak temperature of tan δ. The T_g is higher than the result obtained by DSC and lower than that of PP-DDS [23]. The difference in T_g between PP-DDE and PP-DDS can be ascribed to the

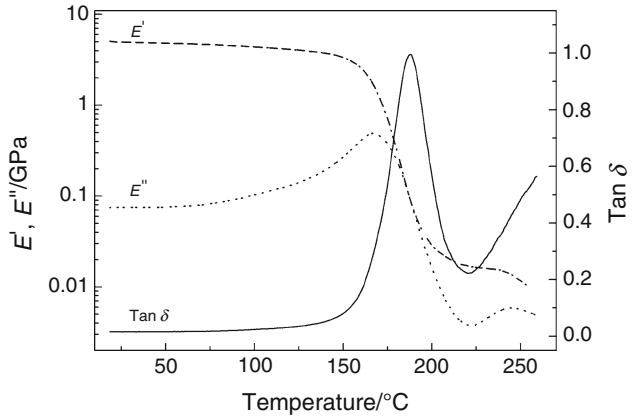

Fig. 6 Dynamic mechanical curves of PP-DDE

different flexibility of the molecular chains between PP-DDE and PP-DDS. In general, tan δ is an important parameter related to the impact resistance of materials, the values of the peak temperature and height of the tan δ of PP-DDE indicate that the molecular mobility and damping characteristics are better than those of PP-DDS. The variation of E', E'', and tan δ with temperature are the response of molecular chain segment motion of PP-DDE in different temperature ranges. In the glassy region, the chain segments of PP-DDE are in a frozen state, and highly immobile, which results in high E' and low E'' values. As temperature increases, some small segments begin to move, and the energy dissipated by the friction between PP-DDE chains begins to increase. Correspondingly, E' decreases and E'' increases gradually. When the temperature reaches the T_g, E'' and tan δ attain a peak value, while E' appears a sharp fall owing to the rapidly increased chain segmental mobility of PP-DDE.

In addition, the values of E' and tan δ of PP-DDE are different from those of the previous reports [21, 22]. The E' at room temperature and the peak height of tan δ are higher than the previous reports, while the peak temperature of tan δ is lower than the previous reports. So, the PP-DDE reported in this paper appears higher flexibility than those of the previous reports. The difference in E' and tan δ between ours and Chang's results may be due to the different preparing processes of PP-DDE, while the difference in E' and tan δ between ours and Qi's results from the different molecular structures, for incorporating cyano-group can enhance the rigidity of polybenzoxazine.

Thermal stability

The TG and the corresponding derivative thermogravimetry (DTG) curves of PP-DDE in air and in nitrogen are shown in Fig. 7. As can be seen, different mass loss behaviors appear in air and in nitrogen. The degradation reaction of PP-DDE shows a multi-step mass loss process

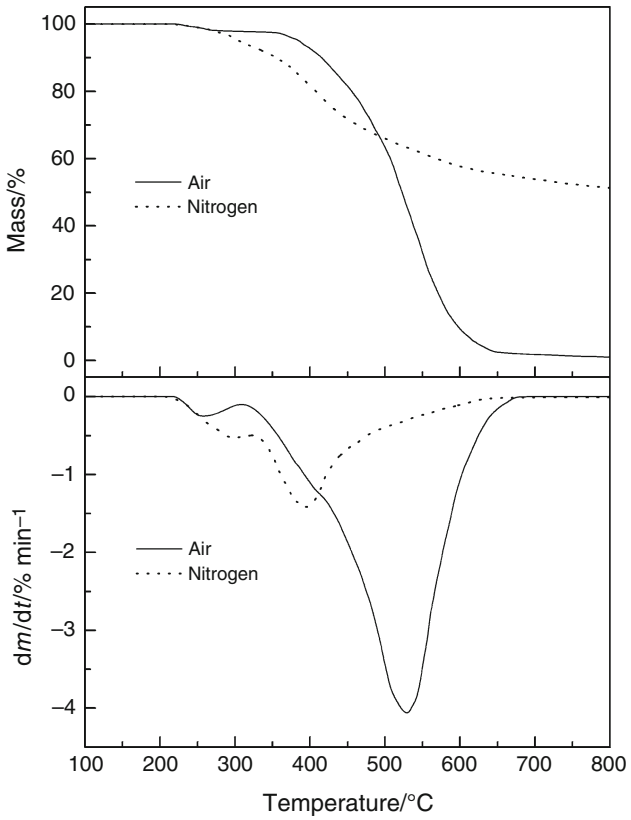

Fig. 7 TG and DTG curves of PP-DDE in air and in nitrogen at a heating rate of 10 °C min^{-1}

in both air and nitrogen. The 10 % mass loss temperature is 353 °C in nitrogen, while 415 °C in air. The char yield is about 48 % at 800 °C in nitrogen, and element analysis for the char shows that the contents of carbon, hydrogen, nitrogen, and oxygen are 83.93, 1.73, 5.48, and 8.85 %, respectively. However, the degradation residue is close to 0 % at 650 °C in air.

In addition, the amount of the mass loss in air and nitrogen are equal at the same temperature from 233 to 277 °C, which indicates that the initial reaction in the degradation is not affected by the atmospheres. With the temperature rising, however, the amount of the mass loss in air is less than that in nitrogen at the same temperature, till temperature reaches about 492 °C. Again, at 492 °C, the amount of the mass loss reaches the same value, 33 %, in both air and nitrogen. Thereafter, the amount of the mass loss in air is more than that in nitrogen at the same temperature. Element analysis shows that the contents of carbon, hydrogen, nitrogen, and oxygen are 80.09, 3.78, 6.04, and 10.09 % for the degradation residue at 492 °C in nitrogen, respectively, while 66.24, 1.97, 7.12, and 24.67 % for the degradation residue at 492 °C in air, respectively. These data indicate that oxidation reaction occurs in the thermal degradation of PP-DDE in air, and owing to the combination of oxygen with PP-DDE in the

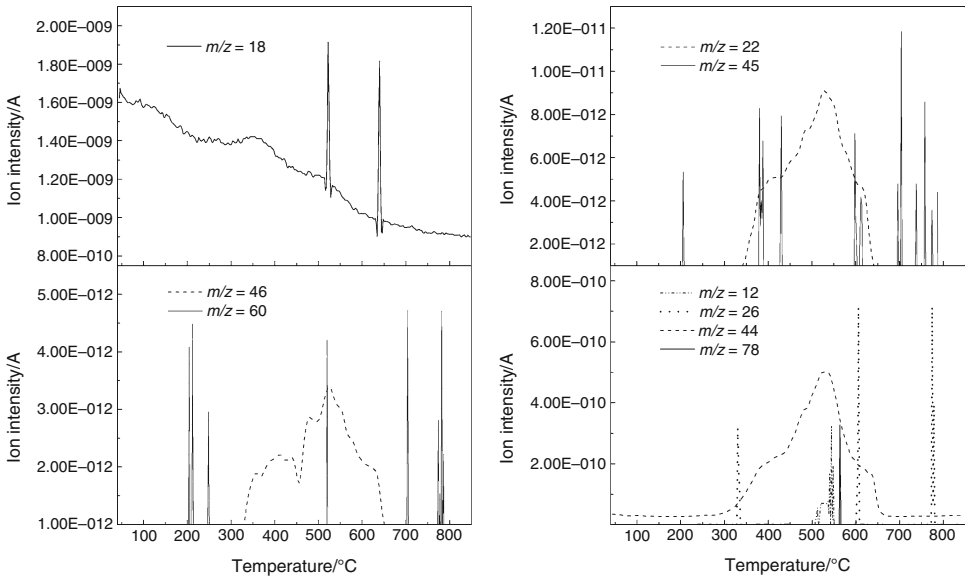

Fig. 8 Ion evolution profiles of the gaseous products detected in thermal degradation of PP-DDE in air

Table 2 The relative abundance of some ions calculated from the peak areas

m/z	12	18	22	26	42	44	46
Relative abundance	0.02123	0.08003	0.00565	0.02425	0.00019	0.86632	0.00228

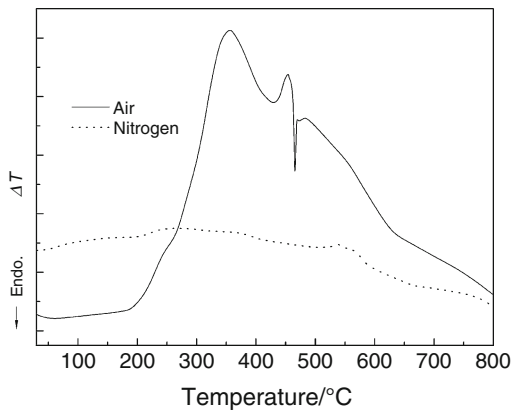

Fig. 9 DTA curves of PP-DDE in air and in nitrogen at a heating rate of 10 °C min^{-1}

early stage of the oxidation reaction, the mass loss in air is less than that in nitrogen at the same temperature between 277 and 492 °C. So, the different mass loss behaviors in air and nitrogen are ascribed to the effect of oxidation.

Owing to the thermo-oxidation, several oxidation gaseous products were evolved in the degradation, which can be seen from the ion evolution profiles detected in thermal degradation of PP-DDE in air shown in Fig. 8. Calculated from the peak areas of the evolved ions, the relative abundances of some ions are listed in Table 2. The assignments of the mass to charge ratio (m/z) for the fragment ions are as follows: m/z = 12 (C^+), m/z = 18 (H_2O^+), m/z = 22 (CO_2^{2+}), m/z = 26 (CN^+), m/z = 44 (CO_2^+), m/z = 45 ($^{13}CO_2^+$), m/z = 46 (NO_2^+), m/z = 60 (CH_2ONO^+), m/z = 78 ($C_6H_6^+$). As can be seen from Fig. 8 and Table 2, the gaseous products mainly consist of CO_2, besides, a little of H_2O, CN^+, and C^+, and trace of NO_2, CH_2ONO, and C_6H_6 released at different temperature ranges in the whole degradation process. The species and amount of the evolved gaseous products indicate that the degradation reaction of PP-DDE in air is thermo-oxidative in nature, and the evolution temperature range of the CO_2^+ corresponds to the temperature region covered by the higher peak in the DTG curve in air. It can be deduced that the H_2O and CO_2 are the resultants of the oxidation of CH_2 of the Mannich bridge structures and the aromatic rings in PP-DDE, while NO_2 and CH_2ONO are evolved due to the oxidation of the Mannich bridge structure.

The DTA curves of PP-DDE in nitrogen and air are shown in Fig. 9. It can be clearly seen that the degradation process of PP-DDE is an exothermic reaction in both air and nitrogen. Due to the presence of oxygen, the thermo-oxidation in air is more complicated than the thermal degradation in nitrogen.

Conclusions

In the thermally activated ring-opening polymerization of benzoxazine based on phenol and DDE, the C–O–C absorption peak of the oxazine ring at 1054 cm^{-1}

disappeared first, and the C–N–C absorption intensity of the oxazine ring decreased gradually with time rising. The activation energies of the non-isothermal polymerization are 83.4 and 87.4 kJ mol^{-1} evaluated with Kissinger and Flynn–Wall–Ozawa methods, respectively. The glass transition temperature of the resultant polybenzoxazine is 188 °C. In the thermal degradation, the 10 % mass loss temperature of the polybenzoxazine is 353 °C and the char yield is about 48 % at 800 °C in nitrogen, while 415 °C and close to 0 % at 650 °C in air.

Acknowledgments This study was financially supported by the Natural Science Foundation of Hebei University (2011YY06).

References

1. Holly FW, Cope AC. Condensation products of aldehydes and ketones with *o*-aminobenzyl alcohol and *o*-hydroxybenzylamine. J Am Chem Soc. 1944;66:1875–9.
2. Burke WJ, Weatherbee C. 3,4-Dihydro-1,3,2H-benzoxazines. Reaction of polyhydroxybenzenes with **N**-methylolamines. J Am Chem Soc. 1950;72:4691–4.
3. Burke WJ, Stephens CW. Monomeric products from the condensation of phenol with formaldehyde and primary amines. J Am Chem Soc. 1952;74:1518–20.
4. Burke WJ, Murdoch KC, Ec G. Condensation of hydroxyaromatic compounds with formaldehyde and primary aromatic amines. J Am Chem Soc. 1954;76:1677–9.
5. Burke WJ. 3,4-Dihydro-l,3,2H-benzoxazines. Reaction of *p*-substituted phenols with *N*,*N*-dimethylolamines. J Am Chem Soc. 1949;71:609–12.
6. Burke WJ, Bishop JL, Glennie ELM, Bauer WN. A new aminoalkylation reaction. Condensation of phenols with dihydro-1,3-aroxazines. J Org Chem. 1965;30:3423–7.
7. Burke WJ, Glennis ELM, Weatherbee C. Condensation of halophenols with formaldehyde and primary amines. J Org Chem. 1964;29:909–12.
8. Ning X, Ishida H. Phenolic materials via ring-opening polymerization: synthesis and characterization of bisphenol-A based benzoxazines and their polymers. J Polym Sci Part A. 1994;32:1121–9.
9. Ning X, Ishida H. Phenolic materials via ring-opening polymerization of benzoxazines: effect of molecular structure on mechanical and dynamic mechanical properties. J Polym Sci Part B. 1994;32:921–7.
10. Liu YF, Yue ZQ, Gao JG. Synthesis, characterization, and thermally activated polymerization behavior of bisphenol-S/aniline based benzoxazine. Polymer. 2010;51:3722–9.
11. Liu J, Agag T, Ishida H. Main-chain benzoxazine oligomers: a new approach for resin transfer moldable neat benzoxazines for high performance applications. Polymer. 2010;51:5688–94.
12. Jia K, Xu MZ, Zhao R, Liu XB. Chemically bonded iron carbonyl for magnetic composites based on phthalonitrile polymers. Polym Int. 2011;60:414–21.
13. Chen KC, Li HT, Chen WB, Liao CH, Sun KW, Chang FC. Synthesis and characterization of a novel siloxane-imide-containing polybenzoxazine. Polym Int. 2011;60:436–42.
14. Li SF, Wang LL. Curing behavior of 4,4′-diamonodiphenyl methane-based benzoxazine oligomers/bisoxazoline copolymers and the properties of their cured resins. J Appl Polym Sci. 2006;99:1359–66.
15. Lin CH, Chang SL, Hsieh CW, Lee HH. Aromatic diamine-based benzoxazines and their high performance thermosets. Polymer. 2008;49:1220–9.
16. Spontón M, Larrechi MS, Ronda JC, Galià M, Cádiz V. Synthesis and study of the thermal crosslinking of bis(m-aminophenyl) methylphosphine oxide based benzoxazine. J Polym Sci Part A. 2008;46:7162–72.
17. Andronescu C, Gârea SA, Deleanu C, Iovu H. Characterization and curing kinetics of new benzoxazine monomer based on aromatic diamines. Thermochim Acta. 2012;530:42–51.
18. Chozhan CK, Alagar M, Gnanasundaram P. Synthesis and characterization of 1,1-bis(3-methyl-4-hydroxy phenyl)-cyclohexane polybenzoxazine–organoclay hybrid nanocomposites. Acta Mater. 2009;57:782–94.
19. Lin CH, Lin HT, Sie JW, Hwang KY, Tu AP. Facile, one-pot synthesis of aromatic diamine-based phosphinated benzoxazines and their flame-retardant thermosets. J Polym Sci Part A. 2010;48:4555–66.
20. Lin CH, Chang SL, Shen TY, Shih YS, Lin HT, Wang CF. Flexible polybenzoxazine thermosets with high glass transition temperatures and low surface free energies. Polym Chem. 2012;3:935–45.
21. Chang SL, Lin CH. Facile, one-pot synthesis of aromatic diamine-based benzoxazines and their advantages over diamines as epoxy hardeners. J Polym Sci Part A. 2010;48:2430–7.
22. Qia HM, Ren H, Pan GY, Zhuang YQ, Huang FR, Du L. Synthesis and characteristic of polybenzoxazine with phenylnitrile functional group. Polym Adv Technol. 2009;20:268–72.
23. Agag T, Jin L, Ishida H. A new synthetic approach for difficult benzoxazines: preparation and polymerization of 4,4′-diaminodiphenyl sulfone-based benzoxazine monomer. Polymer. 2009;50:5940–4.
24. Ishida H, Rodriguez Y. Curing kinetics of a new benzoxazine-based phenolic resin by differential scanning calorimetry. Polymer. 1995;36:3151–8.
25. Russell VM, Koenig JL, Low HY, Ishida H. Study of the characterization and curing of benzoxazines using ^{13}C solid-state nuclear magnetic resonance. J Appl Polym Sci. 1998;70:1413–25.
26. Wang YX, Ishida H. Cationic ring-opening polymerization of benzoxazines. Polymer. 1999;40:4563–70.
27. Wang YX, Ishida H. Synthesis and properties of new thermoplastic polymers from substituted 3,4-dihydro-2H-1,3-benzoxazines. Macromolecules. 2000;33:2839–47.
28. Dunkers J, Ishida H. Vibrational assignments of 3-alkyl-3,4-dihydro-6-methyl-2H-1,3-benzoxazines in the fingerprint region. Spectrochim Acta. 1995;51A:1061–74.
29. Kim HJ, Brunovska Z, Ishida H. Synthesis and thermal characterization of polybenzoxazines based on acetylene-functional monomers. Polymer. 1999;40:6565–73.
30. Su YC, Yei DR, Chang FC. The kinetics of B-a and P-a type copolybenzoxazine via the ring opening process. J Appl Polym Sci. 2005;95:730–7.
31. Agag T, Takeichi T. Preparation, characterization, and polymerization of maleimidobenzoxazine monomers as a novel class of thermosetting resins. J Polym Sci Part A. 2006;44:1424–35.
32. Kissinger HE. Reaction kinetics in differential thermal analysis. Anal Chem. 1957;29:1702–6.
33. Flynn JH, Wall LA. A quick, direct method for the determination of activation energy from thermogravimetric data. J Polym Sci Part B. 1966;4:323–8.
34. Ozawa T. A new method of analyzing thermogravimetric data. Bull Chem Soc Jpn. 1965;38:1881–6.
35. Liu YF, Zhang J, Liu Z, Li ZH, Yue ZQ. Thermally activated polymerization behavior of bisphenol-*S*/methylamine-based benzoxazine. J Appl Polym Sci. 2012;124:813–22.
36. Ishida H, Rodriguez Y. Catalyzing the curing reaction of a new benzoxazine based phenolic resin. J Appl Polym Sci. 1995;58:1751–60.